Numerical investigation of the expansion devices applied in modern vapour compression refrigeration unit considering specific entropy and entropy generation analyses.

Fingas R.[a,b], Haida M. [a], Smolka J. [a], Besagni G. [b], Palacz M. [a], Bodys J. [a], Nowak A. [a]

(a) Department of Thermal Technology, Silesian University of Technology, Konarskiego 22, 44-100 Gliwice, Poland

(b) Department of Energy, Politecnico di Milano, Via Lambruschini 4a, 20156 Milano, Italy

Introduction and motivation

In the ejector-based refrigeration cycles, it is critical to design the ejector for the specific operating conditions in order to use its full potential and achieve the maximal COP improvement for a given case. Therefore, it is necessary to have a better insight into its operation for a proper optimization. The aim of this study was to perform the entropy generation and specific entropy analysis in the CFD environment of widely applied R744 two-phase ejector. The entropy transport equation implemented to ANSYS Fluent software as a User-Defined Scalar (UDS) ensures both local and global analysis of the entropy generation. Furthermore, it allows to find the location of major entropy generation sources.

Mathematical model

The CFD model used in this study was Homogenous Equilibrium Model approach developed by Smolka et al. (2013) [1]. It is suitable for modelling single-, two-phase and supercritical flows. It is characterized by high mass flow rates accuracy with relative errors below 10% in the area close to and above the critical point for motive nozzle operating conditions. Its application range for best accuracy are supercritical region and subcritical region with pressure above 80 bar. The HEM approach was completed with entropy transport equation derived from work of Sierra-Pallares et al. (2016) [2] which has been restructured as an additional transport equation. The entropy generation module was be implemented in the Ansys Fluent using UDS feature:

$$\rho\frac{\delta \mathrm{s}}{\delta \mathrm{t}}+\rho\nabla|(\mathrm{v}\cdot \mathrm{s})-\Gamma_{\mathrm{k}}-\nabla s|=-\nabla\cdot\left(\frac{q}{T}\right)-\frac{1}{T^2}q\nabla T-\frac{1}{T}\tau\colon\nabla\mathrm{v}$$

Since the scope of the research concerns only steady state problems and there is no diffusion of the specific entropy, the above equation can be simplified to the form:

$$\rho\nabla|\mathrm{v}\cdot \mathrm{s}|=-\nabla\cdot\left(\frac{q}{T}\right)-\frac{1}{T^2}q\nabla T-\frac{1}{T}\tau\colon\nabla\mathrm{v}$$

where:

$$\sigma=-\nabla\cdot\left(\frac{q}{T}\right)\qquad\qquad s_g=-\frac{1}{T^2}q\nabla T-\frac{1}{T}\tau\colon\nabla\mathrm{v}$$

The relevant source terms representing the entropy flux vector and each contribution to entropy generation need to be implemented to the UDS by means of the separate source terms written as a C code UDF

Operating conditions

For all cases, the inlet and outlet boundary conditions have been introduced as pressure type boundary conditions with the prescribed pressure and specific enthalpy using the literature data in case of R134a ejector and experimental data in case of the R744 ejector. At the inlet boundary conditions, the specific entropy for UDS equation determined as a function of pressure and temperature was prescribed. At the outlet boundary conditions, the UDF calculating specific enthalpy and specific entropy profiles from neighbouring cell row was prescribed. The mass flow rates were used to validate the numerical model. All cases were simulated as adiabatic with all model walls prescribed with a constant heat flux boundary condition equal to 0. The R134a ejector validation was based on a single operating condition named A-2 from Sierra-Pallares et al. (2016) [2]. The motive inlet conditions were near critical point. The operating conditions for the R744 ejector were based on the results of ejector experimental campaign installed in the transcritical ejector-based R744 refrigeration unit at the Silesian University of Technology.

Table 1: Operating and boundary conditions used for the R134a and R744 ejectors simulations

Case	P_{MN}	T_{MN}	P_{SN}	T_{SN}	P_{OUT}	T_{OUT}	$\dot{M}_{MN}$	$\dot{M}_{SN}$
	bar	°C	bar	°C	bar	°C	kg/h	kg/h
R744 #1	90.7	35.7	27.2	11.6	37.7	3.1	255.7	52.7
R744 #2	76.4	24.8	27.7	4.8	32.0	-3.2	337.7	81.2
R744 #3	79.6	32.4	27.5	8.7	32.3	-2.8	206.4	74.4
R744 #4	90.6	35.4	27.8	10.7	31.7	-3.5	258.0	52.1
R744 #5	88.5	28.2	26.6	6.5	32.2	-2.9	338.2	77.2

Results and discussion

The CFD results of the mass flow rates obtained for the operating conditions were compared with the experimental data. For the cases concerning motive nozzle pressure above 80 bar, the mass flow rates obtained in the numerical model are highly accurate with the relative errors below 10%, meeting the requirements of a good practice in ejector modeling. Cases R744 #2 and #3 are located outside the area of HEM best performance envelope, thus the inaccuracy is high, with the highest error of 35% and 23% for motive and suction nozzle at R744 #2.

Table 2: Mass flow rates of CFD and EXP results with relaitive error for the R744 ejectors simulations.

Case	$\dot{M}_{MN\_EXP}$	$\dot{M}_{MN\_CFD}$	$\dot{M}_{SN\_EXP}$	$\dot{M}_{SN\_CFD}$	$\delta\dot{M}_{MN}$	$\delta\dot{M}_{SN}$
	kg/h	kg/h	kg/h	kg/h	%	%
R744 #1	255.7	270.0	52.7	57.6	6	9
R744 #2	337.7	219.2	81.2	100.8	35	23
R744 #3	206.4	234.0	74.4	82.8	13	11
R744 #4	258.0	280.8	52.1	82.8	9	1
R744 #5	338.2	309.6	77.2	81.0	8	5

The entropy generation in the ejectors takes place mainly through viscous dissipation mechanism, with highest values observed at the mixing section, where supersonic motive stream draws the entrained suction stream, and then decreases velocity along the mixing section where the swirl flow of the suction nozzle is mixing with the core fluid flow. In the case R744 #1 with higher pressure ratio and lower mass entrainment ratio (MER), the majority of the entropy generation takes place at the interface of the motive and suction streams along the mixing section. Cases R744 #2 and R744 #3 indicate strong entropy generation at the premixing section. This can be connected with much higher MER and low pressure ratio. The third entropy generation pattern can be observed at R744 #4 and R744 #5, which indicates the location of entropy generation in both mixing and diffuser sections, where the streams are still mixing in rotating manner. This phenomenon is not visible in field of entropy generation of case R744 #1, for which the entropy is generated throughout the whole mixing section but not in the diffuser.

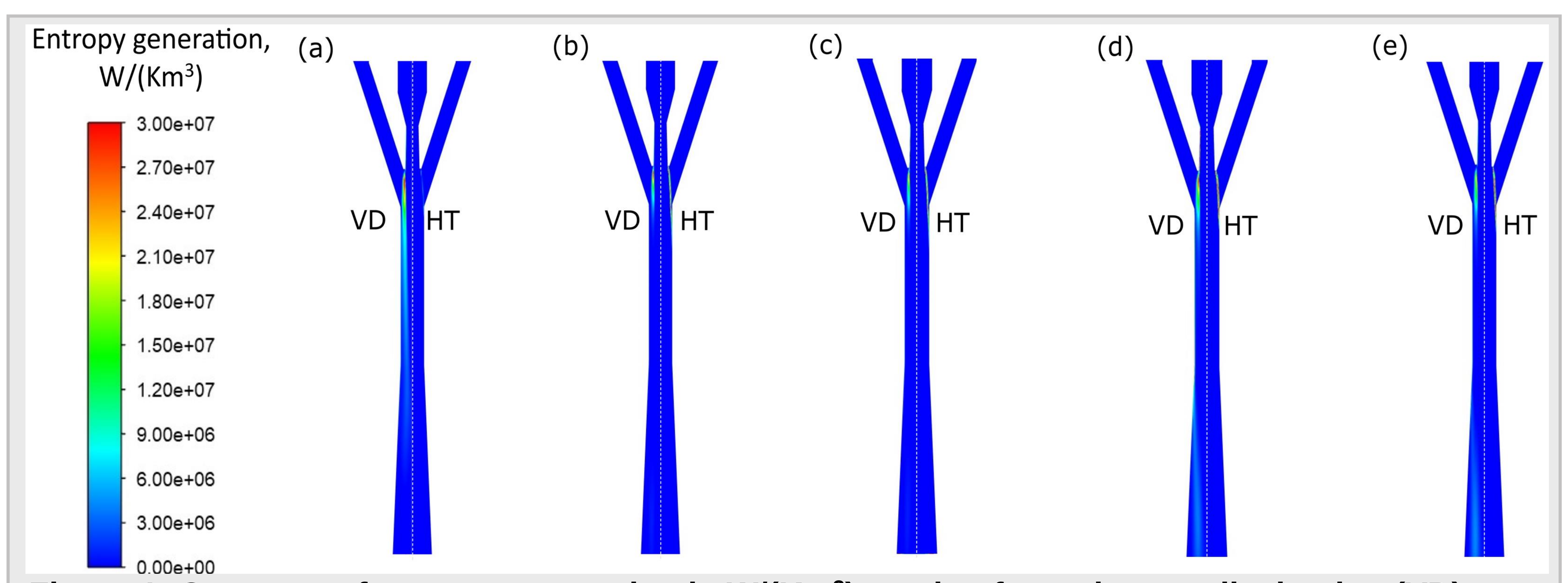

Figure 1: Contours of entropy generation in W/(Km³) coming from viscous dissipation (VD) and heat transfer (HT) sources for cases R744 #1 - #5.

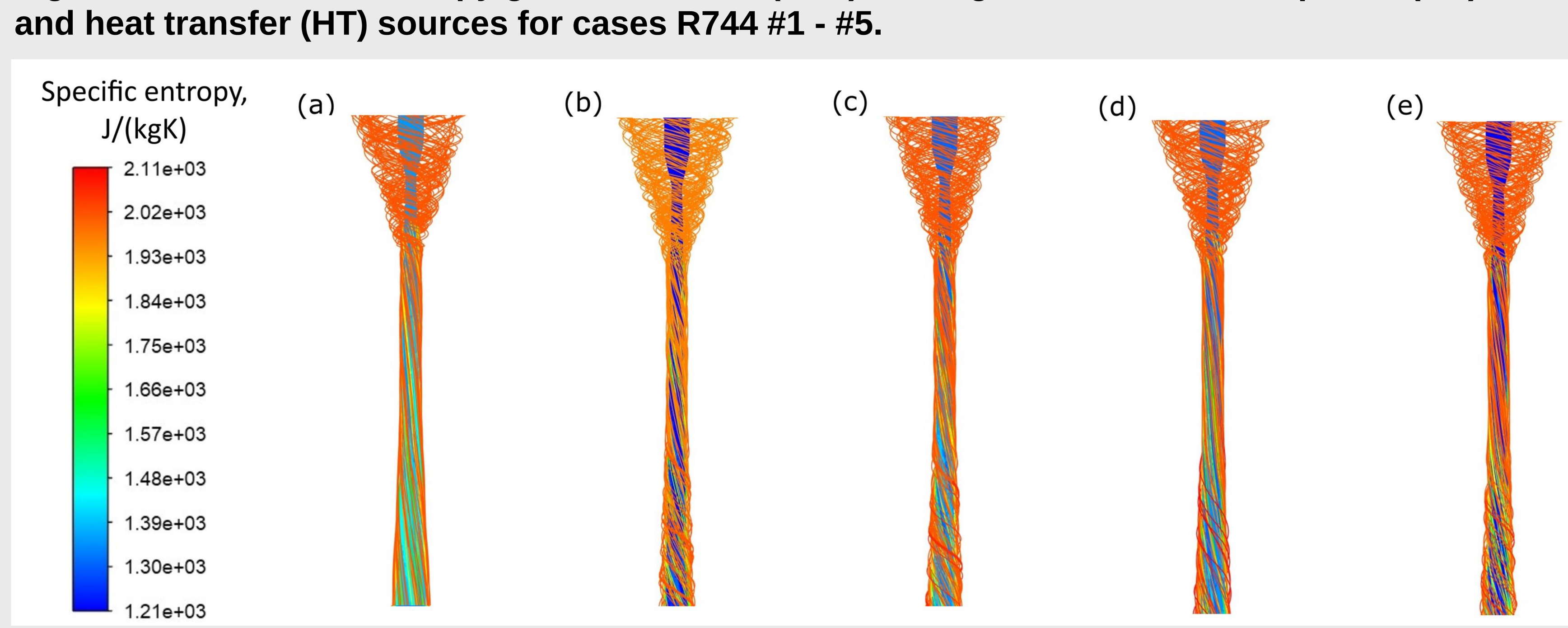

Figure 1: Streamlines of specific entropy in J/(kgK) for cases R744 #1 - #5.

In conclusion, the presented entropy generation fields for the R744 ejector show that the location and value of generation for the same ejector geometry depends on boundary conditions and the mixing intensity. Therefore, higher MER values and velocities impose higher entropy generation caused by viscous forces between suction and motive streams. There was no substantial entropy generation in the vicinity of walls. Additionally, the entropy generation of the R744 ejector occurs mainly in the premixer section and there is no significant generation of entropy in the diffuser section, which was observed for case of R134a single-phase ejector.

[1] Smolka J., Bulinski Z., Fic A., Nowak A.J., Banasiak K., Hafner A., 2013, A computational model of a transcritical R744 ejector based on a homogeneous real fluid approach, Applied Mathematical Modelling, vol. 37, pp. 1208–1224.

[2] Sierra-Pallares J., Garcia del Valle J., Garcia Carrascal P., Castro Ruiz F., 2016, A computational study about the types of entropy generation in three different R134a ejector mixing chambers, International Journal of Refrigeration, vol. 63, pp. 199–213

MSc. Rafal Fingas – rafal.fingas@polimi.it